

High-Frequency Performance of MoS₂ Transistors at Cryogenic Temperatures

Qingguo Gao^{1,2}, Chongfu Zhang^{1,2*}, Zhenfeng Zhang³, Zichuan Yi², Xinjian Pan², Feng Chi², Liming Liu², Xuefei Li³, Yanqing Wu^{3,4*}

¹ School of Information and Communication Engineering, University of Electronic Science and Technology of China, Chengdu 611731, China

² School of Electronic Information, University of Electronic Science and Technology of China, Zhongshan Institute, Zhongshan 528402, China

³ Wuhan National High Magnetic Field Center and School of Optical and Electronic Information, Huazhong University of Science and Technology, Wuhan 430074, China

⁴ Institute of Microelectronics and Key Laboratory of Microelectronic Devices and Circuits (MOE) and Frontiers Science Center for Nano-optoelectronics, Peking University, Beijing 100871, China

* Email: Yanqing Wu (yqw@pku.edu.cn); Chongfu Zhang (cfzhang@uestc.edu.cn)

Abstract

Recently, due to its potential in high-speed flexible electronics, radio-frequency transistors based on two-dimensional MoS₂ has attracted the interest of researchers. However, for the moment, little is known on the RF performance of MoS₂ transistors at cryogenic temperatures, which is important for evaluating performance limits of high-frequency MoS₂ devices. In this work, we report the RF performance of MoS₂ transistors at cryogenic temperatures based on chemical vapor deposited bilayer MoS₂ for the first time. As the temperature reduces, the higher cut-off frequency was achieved. At the liquid helium temperature, extrinsic and intrinsic f_T of 5.7 and 12.7 GHz for the transistor with 300 nm gate-length were achieved. Furthermore, saturation velocity and intrinsic f_{max} of 2.4×10^6 cm/s and 24 GHz were obtained at 4.3 K, respectively. The revealed high-frequency performances of MoS₂ transistors at cryogenic temperatures are helpful to the advancement of MoS₂ high-frequency electronics.

1. Introduction

Recently, the radio-frequency performance of two-dimensional molybdenum disulfide has attracted extensive attention due to it is important for future ubiquitous electronics, such as novel flexible rectenna, amplifier, and mixer [1-3]. Exfoliated MoS₂ radio-frequency (RF) transistors with extrinsic f_T/f_{max} of 10.2/14.5 GHz, and CVD MoS₂ RF transistors with extrinsic f_T/f_{max} of 7.2/23 GHz have been demonstrated by different groups [1, 4]. Zhang *et al.* presented a flexible and multifunction Wi-Fi-band rectenna based on MoS₂ Schottky diodes with a well-designed source and drain contact electrodes [3]. In modern society, many interesting physics phenomena were observed at low temperatures and a number of applications require cryogenic operation. However, no MoS₂ RF transistors have been operated and studied at cryogenic

temperatures [5].

In this work, we carried out the first study of MoS₂ RF transistors down to liquid helium temperatures. The transconductance was obviously improved with the temperature reducing from 250 K down to 4.3 K. As the temperature reduced to 4.3 K, extrinsic cut-off frequency f_T increased from 3.2 GHz to 5.7 GHz and intrinsic f_T increased from 5.7 to 12.9 GHz for the transistor with gate length of 300 nm, and a maximum $f_T \cdot L_g$ of 3.87 GHz· μ m was achieved.

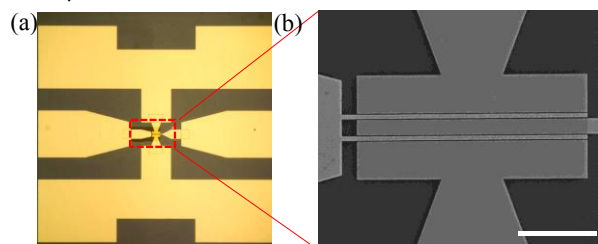


Figure 1. (a) Optical microscopy of the fabricated MoS₂ RF transistor. (b) SEM image of the two-finger top-gated MoS₂ RF transistor with 300 nm gate length. Scale bar 5 μ m.

2. Experimental

Chemical vapor deposited bilayer MoS₂ was grown on molten glass at about 830 °C. Using PMMA as a protective layer, the MoS₂ film was transferred onto high-resistance silicon substrate with atomic layer deposited HfLaO. Excess MoS₂ outside the channel and contacts was etched using O₂/Ar plasma. Then, the source and drain S/D contacts consist of 20 nm Ni flim and 60 nm Au film was fabricated using electron-beam lithography (EBL) and electron-beam evaporation (EBE). The top gate dielectric layer is composed of 6 nm naturally oxidized Al₂O₃ and 11 nm atomic layer deposited HfO₂. At last, top-gate electrodes were formed as the same process as S/D electrodes with 20/60 nm Ni/Au. Here, a two-finger top gate structure with an

underlap arrangement was adopted to improve the current transport as well as to reduce parasitic capacitances between top-gate and S/D electrodes [6]. Figure 1a shows an optical microscope of the fabricated MoS₂ RF transistor with the ground-signal-ground (GSG) configuration. The standard GSG pads were designed to transmit the high-frequency signal from microwave coaxial cables to the MoS₂ RF transistor with coplanar waveguide electrodes. Figure 1b displays the SEM image of the two-finger top-gated MoS₂ transistor with $L_{\text{fg}} = 300$ nm, and the distance between gate and S/D electrodes are about 75 nm.

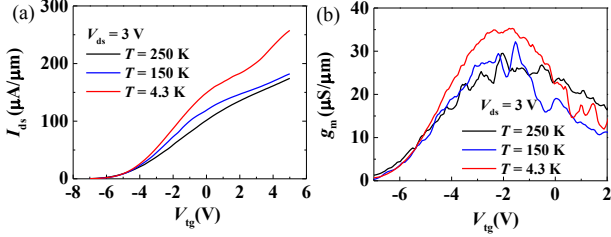


Figure 2. (a) Transfer characteristics ($I_{\text{ds}}-V_{\text{tg}}$) of the MoS₂ device at cryogenic temperatures. (b) The corresponding transconductance g_{m} of the device.

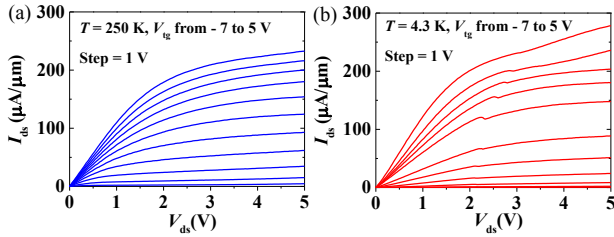


Figure 3. Output characteristics ($I_{\text{ds}}-V_{\text{ds}}$) of the same MoS₂ device at 250 K(a) and 4.3 K(b).

3. Results and Discussion

Using the Lakeshore probe station and the Agilent B1500A semiconductor parameter analyzer, the DC characterization of the MoS₂ transistors at cryogenic temperatures was performed. Figure 2a shows the transfer characteristics ($I_{\text{ds}}-V_{\text{gs}}$) of the 300-nm MoS₂ RF transistors at high drain bias of 3 V from 250 K to 4.3 K. The on-current at $V_{\text{gs}} = 5$ V increases from 174 $\mu\text{A}/\mu\text{m}$ to 257 $\mu\text{A}/\mu\text{m}$ with temperature reduced from 250 to 4.3 K. The corresponding transconductance dependence on gate voltage was shown in Figure 2b, and the highest transconductance of 35 $\mu\text{S}/\mu\text{m}$ at 4.3 K was achieved. These improvements in on-current and transconductance could be attributed to the reduced phonon scattering from the underlying substrate with temperature reduction [7]. Figures 3a and 3b show the $I_{\text{ds}}-V_{\text{ds}}$ curves at 250 K and 4.3 K at different gate voltages of the 300-nm MoS₂ RF transistors, respectively. A clear current density improvement in 4.3 K could be observed, which is consistent with the transfer characteristics.

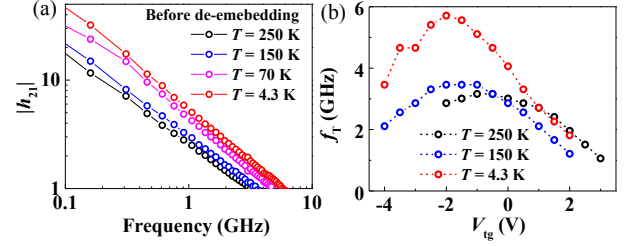


Figure 4. (a) Measured current gain $|h_{21}|$ of the MoS₂ RF transistor at cryogenic temperatures. (b) The dependence of cut-off frequency f_{T} with gate voltage V_{tg} at different temperatures.

In order to characterize the RF performance of MoS₂ transistors at low temperatures, we used Lakeshore cryogenic probe stations and Agilent N5225A vector network analyzers to perform standard on-chip S-parameter measurements. Before S-parameter measurements, standard short-open-load-through (SOLT) calibration method was adopted to calibrate-out the response of the network analyzer, cables, and probes. Then, cut-off frequency f_{T} of the MoS₂ RF transistors at cryogenic temperatures can be obtained. Cut-off frequency corresponds to the maximum frequency with current gain, and which is an important quality factor to evaluate the high-frequency performance of RF transistors. Mathematically, it can be expressed as

$$|h_{21}(f = f_{\text{T}})| = 1 \quad (1)$$

where $|h_{21}(f)|$ represents the relationship between the current gain and frequency. And $|h_{21}(f)|$ can be obtained from the measured Y-parameters of the transistors.

$$h_{21}(f) = \frac{Y_{21}(f)}{Y_{11}(f)} \quad (2)$$

Measured extrinsic $|h_{21}(f)|$ characteristics of the MoS₂ RF transistor at several cryogenic temperatures are shown in Figure 4a. The corresponding peak cut-off frequencies at 250 K, 150 K, 70 K, and 4.3 K are 3.2 GHz, 3.5 GHz, 4.7 GHz, and 5.7 GHz, respectively. There is approximately an 80% improvement in f_{T} at 4.3 K. This improvement can be attributed to the higher carrier mobility and saturation velocity at a lower temperature due to the reduced scattering from both surface phonons and interface traps [1, 8]. Figure 4(b) shows the plot of f_{T} versus gate voltage (V_{tg}) at different temperatures. It can be found that the high-frequency operation of the MoS₂ transistor at different temperatures is highly dependent on the dc bias condition. The f_{T} of a MoS₂ RF transistor can be expressed with

$$f_{\text{T}} = \frac{g_{\text{m}}}{2\pi[(C_{\text{gs}} + C_{\text{gd}}) \cdot (1 + (R_{\text{s}} + R_{\text{d}})g_{\text{o}}) + C_{\text{gd}} \cdot g_{\text{m}} \cdot (R_{\text{s}} + R_{\text{d}})]} \quad (3)$$

where R_{s} and R_{d} are the source and drain access resistances, g_{o} is the output conductance, g_{m} is the transconductance, C_{gs} and C_{gd} are the gate-source and gate-drain capacitances, respectively [9]. As shown in

Figures 2b and 4b, a strong correlation between g_m and f_T can be observed, which is consistent with formula (3).

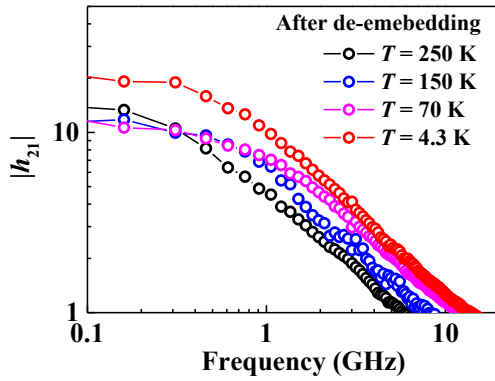


Figure 5. The short-circuit current gain $|h_{21}|$ after standard deembedding of the 300 nm MoS₂ RF transistor at cryogenic temperatures.

In order to obtain the intrinsic frequency performance of MoS₂ transistors, the standard de-embedding process was performed to minimize the parasitic effects on performance evaluation [10]. The short-circuit current gains of different temperatures after de-embedding are shown in Figure 5. The corresponding intrinsic f_T at 250 K, 150 K, 70 K, and 4.3 K are 5.7 GHz, 7.8 GHz, 11.8 GHz, and 12.9 GHz, respectively. Usually, f_T is inversely proportional to channel length, so the product of frequency and gate length ($f_T \cdot L_g$) is a useful metric to evaluate the high-frequency performance of RF transistor. From the maximum f_T obtained at 4.3 K, a $f_T \cdot L_g$ of 3.87 GHz $\cdot\mu\text{m}$ was demonstrated, which is among the highest range of MoS₂ high-frequency transistors [1]. Furthermore, using the expression $v_{sat} = 2\pi f_T L_g$, carrier saturation velocity of 2.4×10^6 cm/s is obtained. Maximum frequency of oscillation, f_{max} , is another important figure-of-merit for RF transistors. It is the frequency at which the power gain of an RF transistor equal to 1. For the 300-nm MoS₂ transistors, the extrinsic and intrinsic f_{max} extracted at 4.3 K are 16 and 24 GHz, respectively.

4. Summary

In this work, a study of the performance of a 300 nm gate-length MoS₂ transistor at cryogenic temperatures has been presented. Key figure-of-merit f_T has been studied systematically at various temperatures. As the temperature reduces, clear cut-off frequency improvement could be observed, and the highest extrinsic and intrinsic f_T of 5.7 and 12.9 GHz was achieved at 4.3 K. Meanwhile, intrinsic f_{max} of 24 GHz and high experimental saturation velocity of 2.4×10^6 cm/s were demonstrated at liquid-helium temperature. These results clearly demonstrated the potential of MoS₂ transistors in the applications of high-frequency

electronics at cryogenic temperatures and are important to improve the high-frequency performance of MoS₂ transistors.

Acknowledgments

This work was supported in part by Guangdong Basic and Applied Basic Research Foundation under Grant 2019A1515110752, in part by Youth Innovative Talent Project of Guangdong Education Department under Grant 2019KQNCX187, in part by the Natural Science Foundation of China under Grant 61874162, in part by the 111 Project under Grant B18001, and in part by Project for Zhongshan Social Public Welfare Science and Technology under Grant 2019B2007.

References

- [1] Q. Gao, Z. Zhang, X. Xu, *et al.*, *Nature Communications*, vol. 9, no. 1, pp. 4778, (2018).
- [2] D. Akinwande, N. Petrone, and J. Hone, *Nature Communications*, vol. 5, no. 1, pp. 5678, (2014).
- [3] X. Zhang, J. Grajal, J. L. Vazquez-Roy, *et al.*, *Nature*, vol. 566, no. 7744, pp. 368-372, (2019).
- [4] R. Cheng, S. Jiang, Y. Chen, *et al.*, *Nature Communications*, vol. 5, no. 1, pp. 5143, (2014).
- [5] Y. Wu, Y.-m. Lin, A. A. Bol, *et al.*, *Nature*, vol. 472, no. 7341, pp. 74-78, (2011).
- [6] W. Zhu, S. Park, M. N. Yogeesh, *et al.*, *Nano Letters*, vol. 16, no. 4, pp. 2301-2306, (2016).
- [7] X. Li, L. Yang, M. Si, *et al.*, *Advanced Materials*, vol. 27, no. 9, pp. 1547-1552, (2015).
- [8] T. Li, M. Tian, S. Li, *et al.*, *Advanced Electronic Materials*, vol. 4, no. 8, pp. 1800138, (2018).
- [9] P. J. Tasker, and B. Hughes, *IEEE Electron Device Letters*, vol. 10, no. 7, pp. 291-293, (1989).
- [10] H. Wang, X. Wang, F. Xia, *et al.*, *Nano Letters*, vol. 14, no. 11, pp. 6424-6429, (2014).